



Original Research Article

Design, Synthesis and Biological Evaluation of Chromone Fused 1,3,4-Thiadiazoles as Highly Potent Nontoxic Inhibitors of Enoyl-Acyl Carrier Proteins in *M. tuberculosis*

Pawan S Hardas¹, Babasaheb V Kendre^{1*}, Rushikesh B Kendre², Rajashri C Patkulkar¹, Mahadev G Landge¹, Dr. Sudhakar R Bhusare³

^{1*} Post Graduate Research Centre in Chemistry, Vaidyanath College, Parli-Vajinath-431515, Dist. Beed, MS, India

² Maharashtra Institute of Medical Sciences and Research, Latur-413512, MS, India

³ DSM College, Parbhani

Received: 2024-10-20

Accepted: 2024-12-17

Published: 2024-12-18

ABSTRACT

A series of 12 novel chromone fused 1,3,4-thiadiazoles were designed and synthesized via an efficient and convenient synthetic route starting from a 3-formyl chromone. In vitro evaluation of all the derivatives was carried out to demonstrate their inhibitory potential against Mtb. Anti-tubercular evaluation via the MABA assay revealed that compounds 5b, 5d, 5f, 5g and 5h significantly inhibited the Mycobacterium tuberculosis H37Rv strain, with MICs in the range of 3.0-8.0 $\mu\text{g ml}^{-1}$. Moreover, the experimental results demonstrated the excellent anti-tubercular potential of compounds 5d and 5f against Mtb with MICs of 3.0 and 4.0 $\mu\text{g ml}^{-1}$. In addition, molecular docking was performed to determine more favorable molecular interactions with the four target enzymes. Molecular docking and binding energy studies revealed the potential of four selected compounds to bind to the enoyl-acyl carrier protein reductase of Mtb which is involved in the biosynthesis of mycolic acid. Interestingly, the binding energies (-8.50 to -10.08 kcal/mol) of all the selected compounds were found to be greater than that of standard drugs. The chemoinformatics study revealed excellent ADME profiles for all the selected compounds, confirming their importance in the treatment of Mtb.

Keywords: Chromone, Thiadiazole, Anti-Mycobacterium tuberculosis, Minimum inhibitory concentration (MIC), Molecular docking, Topological polar surface area (TPSA), Structure-activity relationships (SARs)

*Corresponding author email address: bvkendre71@gmail.com

Introduction

Since the discovery of *Mycobacterium tuberculosis* (M. tb), a deadly pathogenic bacterium reported by Robert Koch in 1882, continuous efforts have been made at the global level to eliminate tuberculosis [1]. Over the last two centuries, tuberculosis has been the leading infectious disease and the leading cause of death worldwide, with almost a billion people dying from this disease [2]. In 2020, there were an estimated 1.3 million deaths worldwide from tuberculosis. The rate of occurrence has weakened over the last two decades, but the disease burden has remained considerable.

TB causes infection to the lungs and other parts of the body, such as the brain, kidneys, and spine [3]. Diagnosis still remains a major challenge, as a few cases remain undetected after diagnosis. Despite considerable advances in understanding diagnostic technologies, treatments and mechanisms of action, the knowledge gap remains inconsiderable. Hence, TB continues to be the focus of international researchers seeking to develop novel therapeutics to address resistance to the available isoniazid, first-line drug and ethionamide, second-line drugs used to treat MDR-TB [4]. The *Mycobacterium tuberculosis* FAS-II (fatty acid synthase II) has the unique property of producing unusually long-chain fatty acids involved in the biosynthesis of mycolic acids. Consequently, the inhibition of fatty acid synthase II is the key target for new drugs. Resistance development associated with these drugs is due to mutations in the activating enzyme or in the upstream promoter region of InhA [5].

Among heterocyclic compounds, chromones have occupied distinct positions in the field of medicinal chemistry because of their wide natural abundance and great potential to inhibit enzymes responsible for causative diseases [6]. There is a well-known history of natural and synthetic chromone derivatives being used as medicinally active compounds [7]. They have been used in ayurveda since ancient times for the treatment of chronic diseases, including allergies [8], diabetes [9], microbial infections [10], and inflammatory diseases [11] (Figure 1).

Chromones are privileged structures that lead to the generation of novel heterocyclic compounds via reactions with useful substrates [12]. A series of synthetic strategies have been reported for the synthesis of chromones including the VilsmeierHaack reaction [13], the Baker–Venktaraman rearrangement [14], the Claisen condensation [15], the Kostanecki–Robinson reaction [16], the Simonis reaction [17] and the Ruhemann reaction [18].

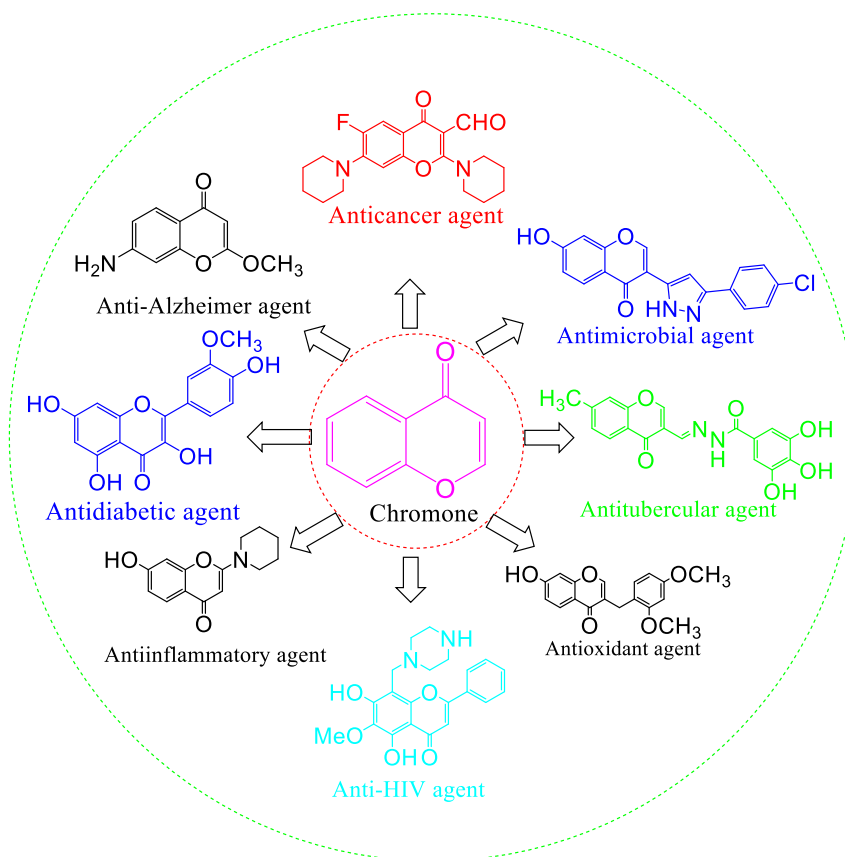


Figure-1: Promising Activities of Chromone fused Heterocyclic Compounds

Recent studies continue to identify novel heterocyclic compounds for therapeutic applications. Among these compounds, 1,3,4-thiadiazoles have been intensely investigated for their practical application in the fields of medicine, agriculture and material science, and many of them are known to possess a broad spectrum of bioactivities, including anti-inflammatory [19], antihypertensive [20], antibacterial [21], antituberculosis [22], anticonvulsant [23], antimicrobial [24], antidepressant [25], antileishmanial [26], and anticancer [27]. A series of drugs in clinical use, including acetazolamide, sulfamethizole, methazolamide, globucid and megazol, have 1,3,4-thiadiazole nuclei (Figure 2). Despite the significant work on thiadiazoles, continuous efforts are still being made to identify novel heterocyclic compounds with potent biological activities. Schiff bases have an interesting range of applications in various fields of science, including medicine and pharmacy, modern technologies, synthesis and chemical analysis [28]. In addition, chromone-fused 1,3,4-thiadiazoles have been reported as potential anticancer agents [29]. In response to the above facts, the present study reports the synthesis of novel Schiff bases from the condensation of 3-formyl chromone with 2-amino-1,3,4-thiadiazoles and investigated their antitubercular activity. The results of molecular docking studies support the activity of the investigated compounds.

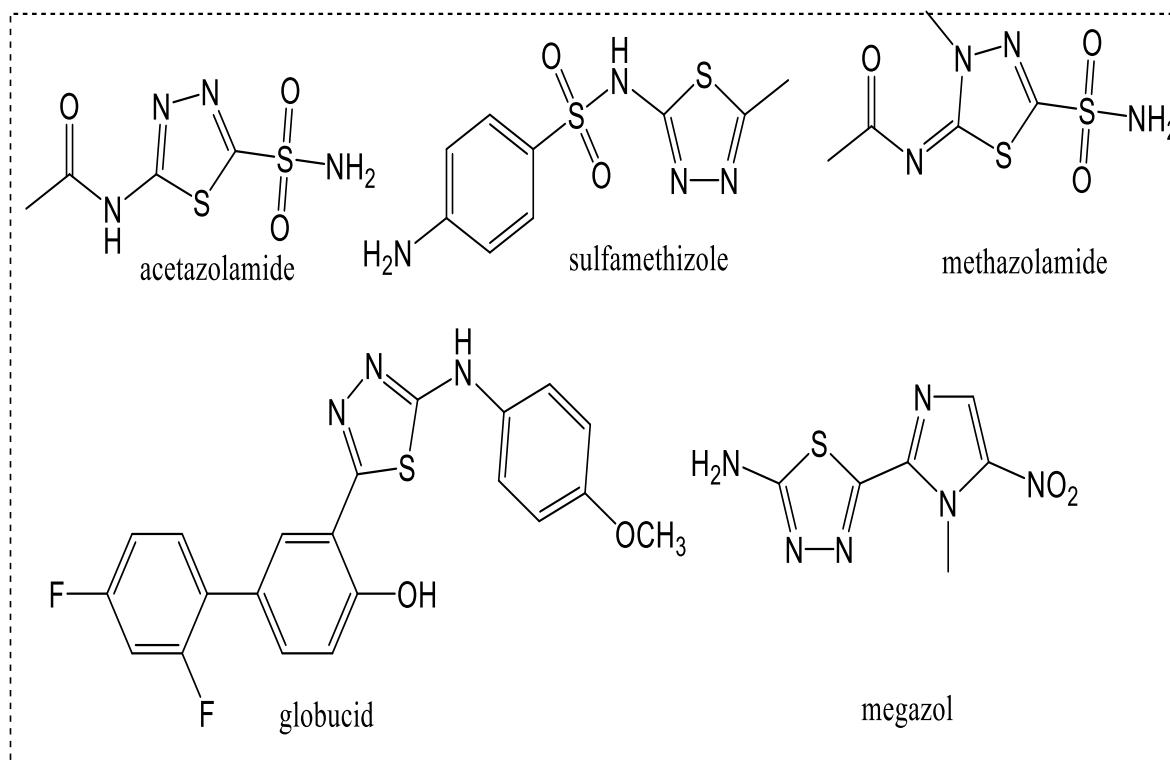


Figure 2: Representative drugs in clinical use that contain 1,3,4-thiadiazole structures

Results and Discussion

Synthesis and Structure

A three-step synthetic strategy was used for the preparation of novel chromone fused 1,3,4-thiadiazoles 5a-l as outlined in Scheme 1. Initially, 3-formyl chromone 4 was prepared from 2-hydroxyacetophenone by the action of Vilsmeier-Haack reagent (POCl₃ in DMF) at 5 °C for half an hour and further at 55 °C for 4 h under stirring in 75% yield. In the second step, 2-aminothiadiazoles 3a-l were prepared from benzoic acids 1a-l and thiosemicarbazide 2 in 75-90% yields at 80-90 °C under refluxing conditions in DMF for 4-5 h. The structures of synthesized intermediate compounds 3a-l were confirmed by IR, ¹H NMR and ¹³C NMR spectral techniques. The conversion of compounds 1a-l into 3a-l upon reaction with thiosemicarbazide 2 was confirmed by thin layer chromatography, functional group tests, melting point calculations, IR, ¹H NMR and ¹³C NMR spectral methods. The disappearance of bands corresponding to acid functional groups between 3000 and 2500 cm⁻¹ and the appearance of N-H stretching bands corresponding to primary amine functional groups in the IR spectrum between 3381 and 3355 cm⁻¹ clearly indicate the conversion of acid into primary amines. The

appearance of bands corresponding to -C=N stretching vibrations in the IR spectrum between 1621 and 1601 supports the structure of compounds 3a-l. The negative esterification test for 3a-l also supports the conversion of acid. Differences in the melting points of the acids and final compounds clearly indicate the formation of amino-1,3,4-thiadiazoles. The disappearance of peaks for carboxyl hydrogen in the ^1H NMR spectra and the appearance of peaks for primary amines in the region of 7.48-7.20 ppm strongly support structures 3a-l. The disappearance of peaks for the carbonyl carbon of the acid functional group in the ^{13}C NMR spectrum for 3a-l confirms the structures, and the characterization data of the ^{13}C NMR spectrum for 3a-l also support the structures. The presence of primary amine groups in 3a-l was detected by a diazotization test. 3-formyl chromone was prepared as per the literature procedure, and its structure was confirmed by functional group tests, mp calculations and ^1H NMR spectral data. Furthermore, 2-aminothiadiazoles were treated with 3-formyl chromone under refluxing conditions in THF for 3-4 h to afford chromone fused 1,3,4-thiadiazole derivatives in 75-82% yield (characterization data and Table 1).

The structures of all the newly synthesized compounds 5a-l were confirmed by IR, ^1H NMR, ^{13}C NMR and mass spectral data (electronic supplementary material). The conversion of 3a-l into 5a-l upon reaction with 3-formyl chromone was confirmed by thin layer chromatography, functional group tests for primary amines and formyl groups and melting point calculations. The disappearance of bands for primary amine and aldehyde groups and the appearance of medium-intensity bands for the azomethine group between 1601 and 1582 cm^{-1} strongly supported the structures of 5a-l. The presence of a single peak in the ^1H NMR spectrum for all target compounds at 7.56 ppm clearly supported the presence of the azomethine group. The disappearance of the peak corresponding to the aldehyde carbonyl carbon in the ^{13}C NMR spectrum of 5a-l fully supported these structures.

The appearance of a number of peaks in the ^{13}C NMR spectrum matches the number of carbon atoms in the target compound. As carbon atoms are present in different chemical environments, peaks are observed at different chemical shift values in the spectrum. The appearance of peaks at approximately $\delta 188\text{ppm}$ in the ^{13}C NMR spectrum for compounds 5a-l clearly suggested the fusion of the chromone scaffold to 1,3,4-thiadiazoles. The EIMS (m/z) values for all synthesized compounds are in good agreement with the molecular weights of the target compounds (refer to the EIMS (m/z) data for 5a-l).

Table 1: Synthesis of chromone-fused 1,3,4-thiadiazole derivatives 5a-l

Entry	R ₁	R ₂	R ₃	R ₄	Reaction Time (h) ^a
5a	H	H	H	H	3.5
5b	OH	H	H	H	4.0
5c	H	NO ₂	H	H	3.0
5d	OH	H	OH	H	3.5
5e	Cl	H	OH	H	4.0
5f	H	OCH ₃	OH	H	3.5
5g	H	OCH ₃	OH	Br	3.0
5h	H	OCH ₃	OCH ₂ COOH	H	3.5
5i	H	OCH ₃	OCOCH ₂ Cl	H	3.5
5j	OCOCH ₃	H	H	H	4.0
5k	H	H	Cl	H	3.5
5l	OH	H	H	NO ₂	3.0

^aReaction time in hours**Anti-mycobacterial evaluation**

Synthesized chromone fused 1,3,4-thiadiazole derivatives (5a-l) were screened for their *in vitro* anti-tubercular activity against *Mycobacterium tuberculosis* H37Rv (ATCC27294) using the Microplate Alamar Blue Assay (MABA assay) method reported by Leonard B³⁰. The minimum inhibitory concentration (MIC; $\mu\text{g ml}^{-1}$) of each compound was studied and compared with that of the standard reference drugs ethambutol and rifampicin. The MIC values for the synthesized compounds and the standard drugs are reported in Table 2. Among the 12

screened derivatives, 5 derivatives (5b, 5d, 5f, 5 g and 5 h) were found to be more active, with MIC values in the range of 3.0-8.0 $\mu\text{g ml}^{-1}$. Derivative 5f was found to be highly potent among all the tested derivatives, with an MIC of 3.0 $\mu\text{g ml}^{-1}$. Derivative 5b and 5d, with MIC values of 5.0 $\mu\text{g ml}^{-1}$ and 4.0 $\mu\text{g ml}^{-1}$, respectively, were found to be closely related to the standard drug ethambutol (MIC, 7.64 $\mu\text{g ml}^{-1}$).

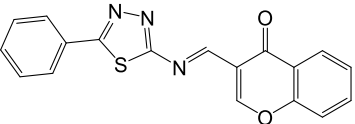
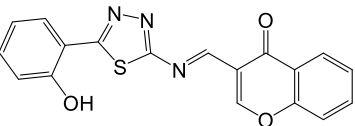
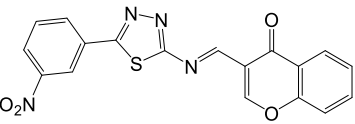
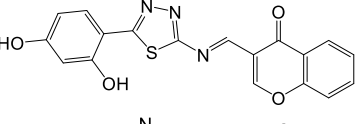
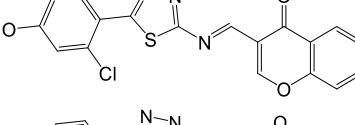
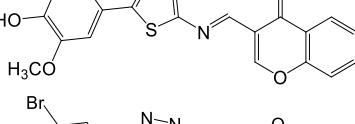
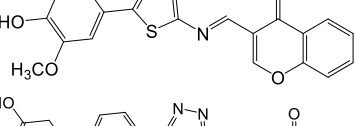
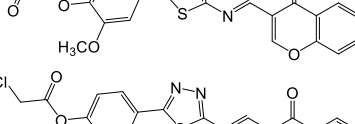
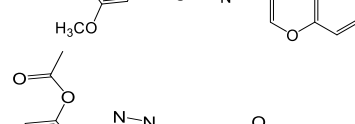
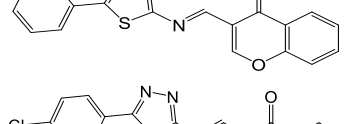
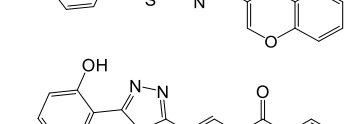
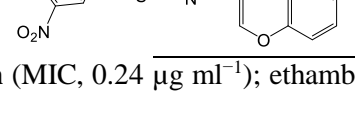
The remaining two derivatives, 5 g and 5 h, exhibited moderate activity with MICs of 6.0 $\mu\text{g ml}^{-1}$ and 8.0 $\mu\text{g ml}^{-1}$ (Table 2). The SAR study of chromone fused 1,3,4-thiadiazole demonstrated that compounds bearing phenyl rings with substituents such as OH, OCH₃, Cl, Br, OCOCH₂Cl, OCH₂COOH, and NO₂ could inhibit *Mycobacterium tuberculosis*.

The experimental cytotoxicity results showed that the selected compounds had cytotoxicity values in the range of 12-20 $\mu\text{g/ml}$, indicating that the compounds are nontoxic. It was also observed that the substitution of the OH group at positions 2 and 4 of the phenyl ring enhances the activity against Mtb. Substitution of the methoxy group at position 3 and the OH group at position 4 greatly enhanced the inhibitory potential against Mtb. However, the substitution of the NO₂ group at position 3 results in a loss of activity. The loss of activity results when the halogens are substituted at positions 2 and 4. The allyl group substitution that replaces the hydrogen from the phenolic OH at position 4 reduces the activity. The loss of activity occurs when an ethyl acetate group is introduced by replacing the hydrogen of the phenolic OH group at position 4. Substitution of position 3 by the OCH₃ group and 4 by the OCOCH₂Cl, -Cl and OCH₂COOH groups reduces the inhibition of Mtb. The loss of activity was observed when the proton of OH at position 2 was replaced by a COCH₃ group.

A loss of activity was also observed when 2-aminothiadiazole and chromone were tested individually against Mtb. The above observations clearly reveal that the bridge (CH=N) formed due to the fusion of two compounds is responsible for enhancing the antitubercular activity. The results also indicate that the nature and position of substituents on chromone fused 1,3,4-thiadiazole structures are very important for identifying potent anti-tuberculosis agents. Importantly, the replacement of the chromone core by an aromatic aldehyde leads to the loss of activity.

The replacement of 2-aminothiadiazole by aromatic primary amines again led to the loss of activity against Mtb.

Table 2: *In vitro* anti-tubercular activity of chromone-fused 1,3,4-thiadiazoles against *Mycobacterium tuberculosis* H37Rv.

Entry	Compound	Assay	MIC ($\mu\text{g ml}^{-1}$) ^a	Activity	(Cytotoxicity) ^b (CC50, $\mu\text{g/ml}$)
5 a		MABA	50	inactive	12
5 b		MABA	5.0	active	18
5 c		MABA	>25	weakly active	nd
5 d		MABA	4.0	active	16
5 e		MABA	>25	weakly active	nd
5 f		MABA	3.0	active	12
5 g		MABA	6.0	active	nd
5 h		MABA	8.0	moderately active	18
5 i		MABA	>25	weakly active	nd
5 j		MABA	32	inactive	nd
5 k		MABA	16	moderately active	20
5 l		MABA	>25	weakly active	nd

^aRifampicin (MIC, $0.24 \mu\text{g ml}^{-1}$); ethambutol (MIC, $7.64 \mu\text{g ml}^{-1}$); ^bCytotoxicity at $50 \mu\text{g/ml}$; nd: Not detected

Computational studies

To study the inhibitory effects of different compounds on *Mycobacterium tuberculosis* via different pathways, we selected 4 validated protein targets, namely, thymidylate kinase (PDB ID: 1G3U), 6,7-dimethyl-8-ribityllumazine synthase (PDB ID: 1W19), enoyl-acyl carrier protein (PDBID: 1W19), and MTB phosphotyrosine phosphatase B (PDB ID: 2OZ5), based on their roles in different pathways (table 3). Thymidylate kinase (TMPK) is an essential enzyme involved in nucleotide metabolism that catalyzes the phosphorylation of thymidine 5'-monophosphate (dTMP) to form thymidine 5'-diphosphate (dTDP) in the presence of ATP and magnesium [31].

TMPK plays a vital role in cell proliferation. Therefore, it has been considered a validated target for rational drug design. Lumazine synthase is an enzyme involved in the biosynthesis of riboflavin and is a highly attractive target for drugs against bacterial infections because the inhibition of this enzyme does not interfere with enzymes involved in mammalian metabolism [32]. The main function of enoyl-acyl carrier protein reductase (InhA) is in the final step of fatty acid biosynthesis, in which 2-trans-enoyl-acyl carrier protein is reduced by utilizing NADH [33]. Among the two protein-tyrosine phosphatases of *Mycobacterium tuberculosis* (Mtb), namely, PtpA and PtpB, PtpB is a triple-specificity phosphatase that plays a crucial role in survival of mycobacteria within the host; because of its secretory nature, it is an attractive drug target for drug design [34].

Methodology:

Preparation of Ligands

The two-dimensional structures of all the compounds were drawn using ChemDraw software, and the designed structures were converted into mol files for further study. The structures were converted to 3-D structures using the LigPrep tool of the Schrödinger suite via the OPLS 300 force field³⁵. The top-ranked ligands were selected for docking purposes.

Preparation of receptor molecules

The protein targets listed in Table 3 were retrieved from the RCSB protein database and prepared according to the literature. The ligand interaction (PDB) file of proteins in complex with inhibitors was downloaded from the protein data bank, and the tool protein preparation wizard of the Schrödinger suite (version 10.3; Maestro, v. 10.3; Schrödinger, LLC, New York,

NY, USA) was used for the preparation of macromolecules. The preprocessing, optimization, and minimization steps were performed using the OPLS 300 force field with an RMSD cutoff value of 0.3 Å. The hydrogen atoms were added at pH 7.0. Grid generation on the receptor was performed using the receptor grid generation tool of the software. The receptor grid was generated at the center of the active site where the key residues are located.

Molecular docking

Molecular docking was performed by using the ligand docking tool of the Schrodinger suite. First, the ligand was prepared using the LigPrep tool of the software via the OPLS 300 force field. LigPrep generates possible 3-D poses of the ligands, ranking them in descending order. The top-ranked pose was selected for docking purposes.

Using a ligand docking tool, the top ranked ligand was allowed to dock with receptor macromolecules. The ligand from the workspace was flexibly docked in a grid box using a Monte Carlo-based simulation algorithm. The binding pose was generated by employing the extra precision (XP) method. Molecular docking of all the designed molecules was performed against protein targets. The docked molecules that exhibited better binding energy and useful interactions with the key residues were selected for synthesis and evaluated against Mtb. The selected docked molecules were ranked according to their binding energy (Table 4).

Molecular docking analysis

To explore the potential targets of the synthesized compounds, we performed docking with four known target proteins reported thus far for chromone-based antitubercular agents. Validated protein targets, such as thymidylate kinase (PDB ID: 1G3U), 6,7-dimethyl-8-ribityllumazine synthase (PDB ID: 1W19), enoyl-acyl carrier protein (PDB ID: 1W19), and MTB phosphotyrosine phosphatase B (PDB ID: 2OZ5), were considered for the study³⁶. The binding modes and conformations of the ligand molecules were studied using automated docking methodology.

A series of 12 chromone fused 1,3,4-thiadiazoles were synthesized and tested against Mtb. Four ligands out of 12 were selected for docking with 4 proteins because they showed significant potential against Mtb. Among the 4 proteins, 1ZID, an enoyl-acyl carrier protein, exhibited better binding scores with four chromone fused 1,3,4-thiadiazoles than did the other proteins (Table 4). Compound 5f was found to have the best score when compared with the

other selected compounds for docking purposes. Its binding score ranged from -5.264 to -10.081 kcal mol⁻¹ for the 4 proteins. Four selected compounds had better docking scores against 1ZID. Therefore, the protein 1ZID was selected, and the details of the binding reports are presented herein. The docking pose of compound 5b with the enoyl-acyl carrier protein is shown in Figure 4. The enoyl-acyl carrier protein reductase (InhA) of the type II fatty acid synthase system is involved in the synthesis of mycolic acids, which are major components of the bacterial cell wall. For these reasons, enoyl-acyl carrier proteins have become popular targets in drug discovery programs.

The intermolecular protein ligand interactions with key residues of the protein are depicted in Figure 2. The docking poses represented in Figure 3 show the intermolecular interactions of compounds 5b, 5d, 5f, and 5 h and the reference drug ethambutol with key amino acids from the active site of the protein (1ZID). Among these compounds, 5f had the highest binding energy value of -10.081 kcal mol⁻¹. Compound 5f exhibited 3H-bond interactions with Ser20 and Gly14 and pi-pi stacking with Phe149. Compound 5d forms 03 H-bond interactions with Ser20, Gly14 and Thr196 and π - π stacking with Phe149. The molecular interactions of compound 5b with key residues were Phe149, Tyr158, Trp222, Ala191, and Thr196 (Table 5).

Notably, the number of molecular interactions between 5b and the key residues is similar to that between the reference drug ethambutol and 5b, with a binding energy of -8.527 kcal mol⁻¹. The above four compounds exhibited similar binding to the native ligand NADH.

Simply put, they have different orientations in the domain of the protein. Compound 5b binds strongly to hydrophobic residues such as Phe149, Gly192, Pro193, Leu218, Tyr158 and Trp222 at the top of the domain, whereas compounds 5d, 5f, and 5 h bind at the bottom of the large open cavity. Interestingly, compounds 5b and 5d possess similar structures, but the only difference is the additional OH group at position 4 in the structure of 5d. Substitution of an additional OH group in compound 5d improved the binding energy score.

The above results suggest that the pi-pi interactions and H-bond interactions improve the docking score of the ligand.

All these compounds were observed to be well bound in the main pocket region of the protein by forming intermolecular interactions with key amino acids. The above observations indicate that all four compounds 5b, 5d, 5f and 5 h may have important effects on the active site of the receptor.

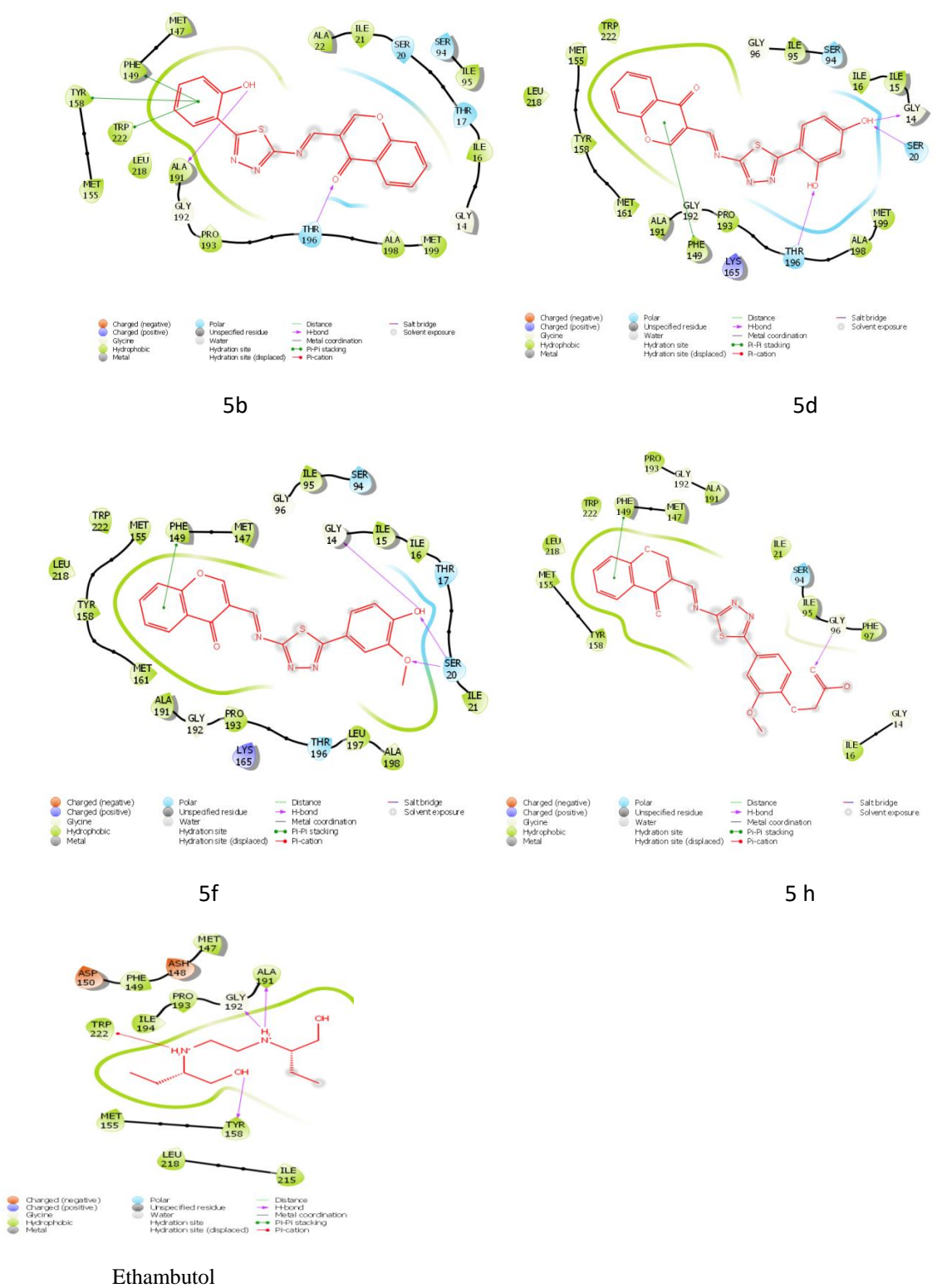


Figure 3: Molecular interactions of compounds 5b, 5d, 5f, and 5 h with ethambutol at the active site of the enzyme 1ZID.

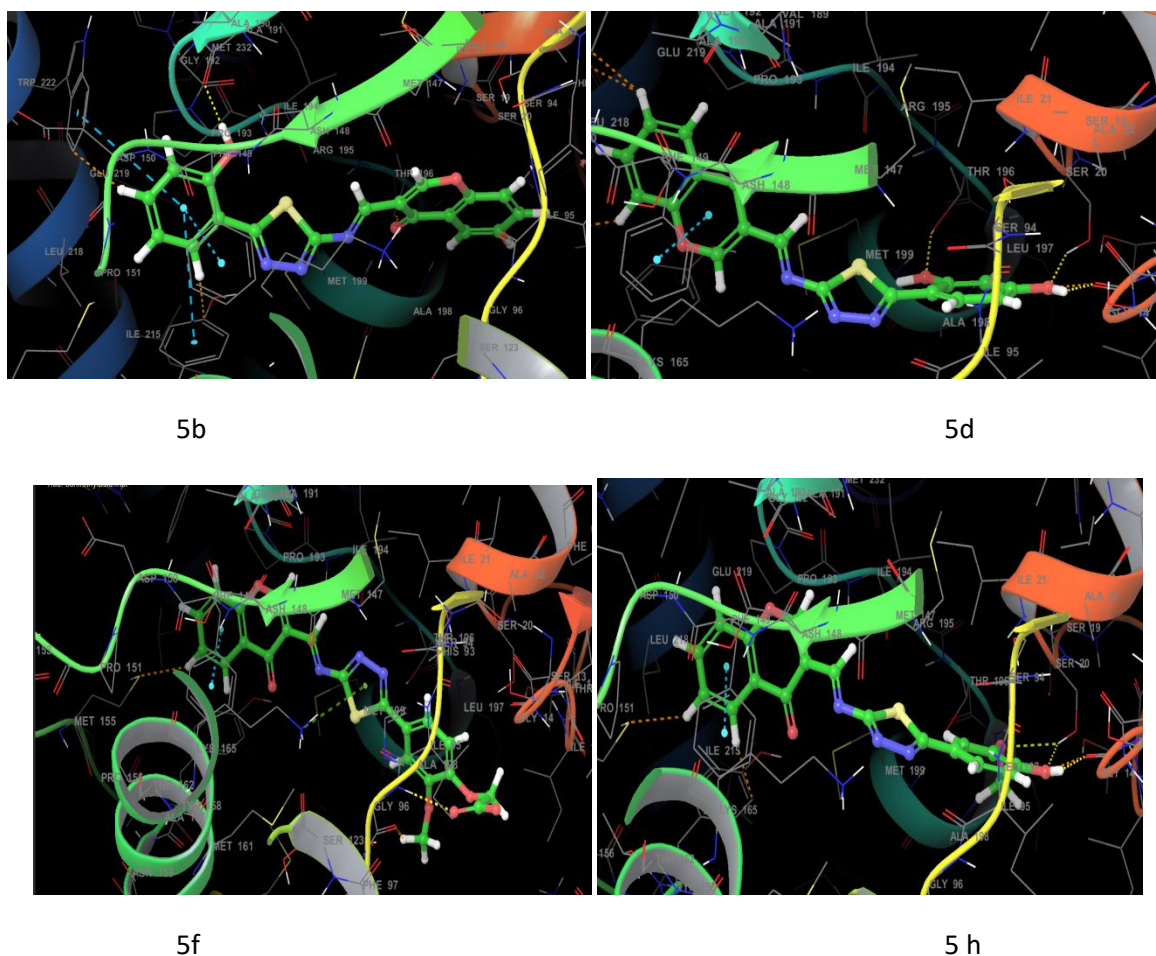


Figure 4: Compounds 5b, 5d, 5f and 5 h in the pocket of the enoyl-acyl carrier protein (PDB ID: 1ZID).

Chemoinformatics analysis

SwissADME, a web tool, was used to study the chemoinformatics of the four selected compounds. The compounds were evaluated for their physicochemical, pharmacokinetic, drug likeness, and medicinal chemistry friendliness properties [37]. The ADME parameters, pharmacokinetic properties, druglike nature and medicinal chemistry friendliness properties were recorded to support drug discovery (Table 6). The Lipinski rule of five was predicted using experimental and computational approaches [38]. According to the Lipinski rule of five, poor absorption or permeation of a drug is possible when it has a high molecular weight, more than 5 H-bond donors and 10 H-bond acceptors.

Literature studies report that solubility and lipophilicity are basic key parameters that determine the success or failure of drug discovery and development [39]. The poor solubility of a compound can lead to reduced productivity. The main challenge during drug discovery is the poor bioavailability of oral dosages. The optimum range of lipophilicity to achieve good

availability is logP in the range of 0-3. A high lipophilicity leads to a high rate of metabolism, which leads to poor solubility and low absorption. The rotatable bonds and ionization states are also very important parameters that predict bioavailability.

The present study highlights the synthesis of drugs that possess excellent physicochemical properties, such as rotatable bonds, H-bond acceptors and donors; solubility and lipophilicity; and good BBB permeability. All the selected compounds had molecular weights less than 500 and abided by the Lipinski rule of five with zero violation. The polar surface area (PSA) is a widely used molecular descriptor tool in the study of drug transport properties, such as intestinal absorption and blood–brain barrier penetration [40]. The topological polar surface area is a significant tool used in virtual screening and for predicting ADME properties, including BBB crossing tendency. The polar surface areas for the selected compounds (5b, 5d, 5f and 5 h) are 116.82, 137.05, 126.05 and 155.18 Å², respectively, indicating that the membrane permeability is very good for the reported compounds.

An experimental cytotoxicity study indicated that all the selected compounds exhibited normal toxicity, as the values were in the range of 10-20 µg/ml.

Table 3: List of tuberculosis targets and mechanistic pathway classes

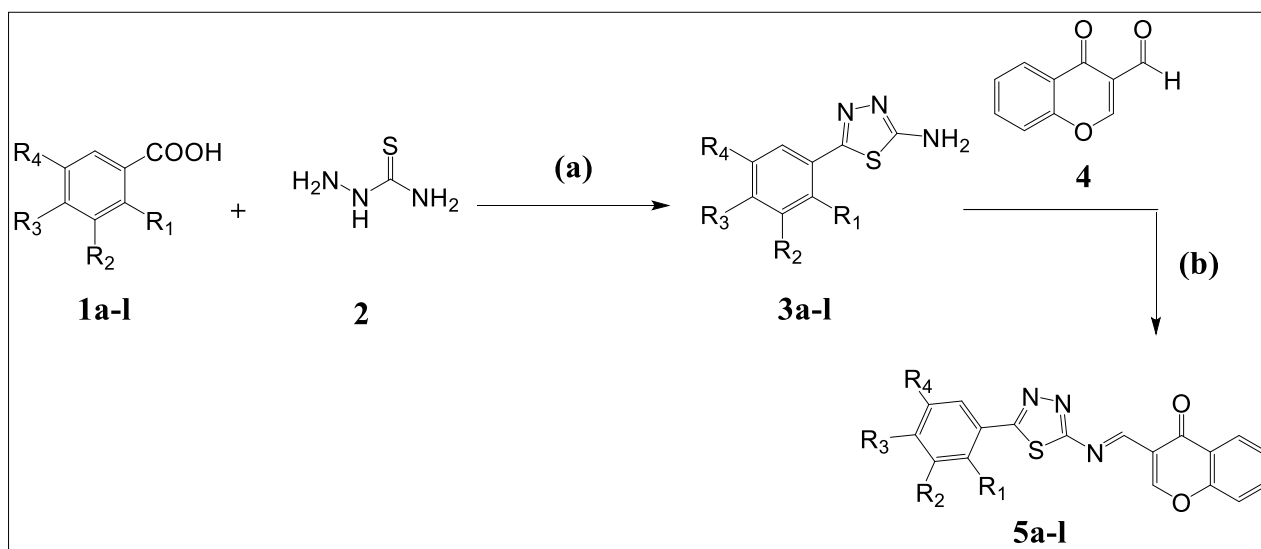
PDB ID	name of targets	mechanistic pathway class
1G3U	thymidylate kinase	DNA synthesis
1W19	6,7-dimethyl-8-ribityllumazine synthase	cofactor biosynthesis
1ZID	enoyl-acyl carrier protein	mycolic acid biosynthesis
2OZ5	MTB phosphotyrosine phosphatase B	arrest of phagosome maturation

Table 4: Molecular docking analysis of 4 protein targets with selected compounds; the binding energies were calculated for Glide in kcal mol⁻¹

PDB Target	Glide score binding energy (kcal/mol ⁻¹)			
	Compound 5b	Compound 5d	Compound 5f	Compound 5 h
1G3U	-5.408	-5.741	-6.988	-5.213
1W19	-1.497	-1.089	-5.264	-1.918
1ZID	-8.527	-9.312	-10.081	-8.506
2OZ5	-4.699	-5.483	-5.879	-5.401

Table 5: Molecular docking of selected compounds with the 1ZID protein

Protein target	Compound	Molecular interactions with key residues	Binding energy kcal/mol ⁻¹
1ZID	5b	Phe149, Tyr158, Trp222, Ala191, Thr196	-8.527
	5d	Phe149, Thr196, Gly14, Ser20	-9.312
	5f	Phe149, Gly14, Ser20	-10.081
	5 h	Phe149, Gly96	-8.506
	ethambutol	Trp222, Tyr158, Ala191, Gly192	-5.545

Scheme 1: Synthesis of Chromone fused 1,3,4-thiadiazoles

Reagents and reaction conditions: a) POCl₃, Reflux, 3-4 h; b) THF, Reflux, 3-4 h

Antitubercular activity

The MABA was used for the screening of synthesized compounds against *Mycobacterium tuberculosis*. It is superior, nontoxic, uses a thermally stable reagent and is correlated with proportional and BACTEC radiometric methods. *M. tuberculosis* was cultured in 7H9 medium supplemented with the synthesized compounds in a 96-well plate at concentrations of 0.8, 1.6, 3.12, 6.25, 12.5, 25, 50 and 100 µg/ml. Sterile deionized water (200 µl) was added to the outer perimeter of the sterile 96-well plates to minimize evaporation of the medium in the test wells during incubation. Then, 100 µl of Middlebrook 7H9 broth was added to the 96-well plate, and

serial dilutions of the test compounds were made on the plate. The final concentration of the drug was 0.2 to 100 $\mu\text{g/ml}$. The plates were covered and sealed with parafilm and incubated at 37 °C for five days. A freshly prepared 1:1 mixture of Almar Blue reagent and 10% tween 80 was added to the plate and incubated for 24 h. The blue color in the well indicates no bacterial growth, and the pink color indicates growth. The calculations were performed on the basis of the percent reduction in dye, which is directly proportional to bacterial growth. The compound was found to be active when the percent reduction in activity of the Almar blue dye was less than the observed value for the standard compounds. The standard drugs rifampicin and ethambutol were used for the study. The results are shown in Table 2.

Table 6: Physicochemical properties of chromone-fused 1,3,4-thiadiazoles

Properties	Compounds				
	5b	5d	5f	5 h	ethambutol
Physicochemical					
MW(g/mol)	349.36	365.36	379.39	436.42	206.33
HBA	6	7	7	9	2
HBD	1	2	1	0	4
nRotb	3	3	4	7	9
TPSA (\AA^2)	116.82	137.05	126.05	155.18	73.68
Lipophilicity					
LogP _{0/w}	3.26	2.93	3.37	2.84	-1.28
Water solubility					
Log S	-4.41	-4.26	-4.46	-4.49	-0.47
Pharmacokinetics					
GI absorption	High	Low	High	Low	Low
BBB permeant	No	No	No	No	No
Druglikeness					
Lipinski	Yes; 0 Violation	Yes;0 violation	Yes; 0 violation	Yes;0 violation	Yes;0 violation
Bioavailability score	0.55	0.55	0.55	0.55	0.55
Medicinal Chemistry					
Leadlikeness (LL)	Yes	MW>350	MW>350	MW>350	Viol. No.2

The molecular weight (MW), log of the octanol/water partition coefficient (logP), hydrogen bond acceptor (HBA), hydrogen bond donor (HBD), topological polar surface area (TPSA), number of rotatable bonds (nRotb), and blood–brain barrier (BBB) penetration were calculated.

Cytotoxicity Assay

A cytotoxicity assay was performed against Vero cells using the MTT assay [41]. For all tested compounds, $\sim 10^3$ cells/well were added to a 96-well plate and incubated at 37 °C in an atmosphere of CO₂ (5%). After incubating for 24 h, the test compound was added at concentrations ranging from 100 to 12.5 µg/mL and further incubated for 72 h. A solution of MTT (3-(4,5-dimethylthiazol-2-yl)-2,5-diphenyltetrazolium bromide) was added to each well and incubated further for 4 h at 37 °C. The residual medium was discarded, 0.1 mL of DMSO was added to dissolve the formazan crystals, and colorimetric measurements were carried out (OD) at a 540 nm filter. Doxorubicin was used as a positive control, and the experiment was repeated twice for accuracy. The CC₅₀ was calculated based on the optical density values. CC₅₀ is the lowest concentration of compound that leads to a 50% reduction in cell viability.

Conclusion

A series of twelve chromone fused 1,3,4-thiadiazoles (5a-l) were designed and synthesized *via* an efficient and convenient synthetic route starting from 3-formyl chromone and screened for their antitubercular activity. An antitubercular screening study revealed the potential of five synthesized compounds against the *Mycobacterium tuberculosis* H37Rv strain. Compounds 5b, 5d and 5f exerted strong inhibitory effects, whereas 5g and 5h had moderate inhibitory effects. Molecular docking studies revealed that compounds 5b, 5d and 5f are more effective against the enoyl-acyl carrier protein reductase of Mtb. Molecular docking and chemoinformatics studies—support the drug likeness of all synthesized compounds. Docking studies indicated pi-pi and H-bond interactions between compound 5b and key residues of the enoyl-acyl reductase protein, namely, Phe149, Tyr158, Trp222, Ala191, and Thr196. Similar interactions were detected with ethambutol. The biological screening results revealed that compound 5f was more potent in this series. The screening results of all synthesized compounds were exactly correlated with the docking results, indicating that molecular docking is a powerful approach for the identification of novel drugs. All synthesized compounds were fully characterized by their IR, NMR and mass spectral data. The SAR study of chromone fused 1,3,4-thiadiazole demonstrated that compounds bearing phenyl rings with different

substituents, such as OH, OCH₃, Cl, Br, OCOCH₂Cl, OCH₂COOH, and NO₂, have good potential to inhibit Mtb.

Experimental Section

Chemicals and methods

All the solvents were freshly distilled before use in chemical transformations. Spectroscopic techniques such as FT-IR (Bruker), ¹H NMR (Bruker AC-400), and ¹³C NMR (Bruker AC-400) were used for the characterization and confirmation of the structures. The ¹H NMR and ¹³C NMR spectra were recorded in DMSO-d₆. The progress of the reactions was monitored using TLC plates coated with silica gel and visualized under a UV lamp. Mass spectra were recorded at ionization energy of 70 eV.

Synthesis of 4-oxo-4*H*-chromene-3-carbaldehyde (4)

A dry solution of POCl₃ (15.3 ml) was added to a solution of DMF (30 ml) in a 250 ml round bottom flask at a temperature of 0-5 °C drop wise with constant stirring for 10 minutes. At the same temperature, the reaction mixture was further stirred for 10 min, after which a solution of 2-hydroxyacetophenone (7.8 gm) in DMF (10 ml) was added drop wise. The reaction mixture was further stirred for 40 min at room temperature and refluxed in a water bath for 4 h. The progress of the reaction was monitored by TLC. After completion of the reaction, the reaction mixture was cooled to room temperature and poured into ice-cold water (250 ml). The contents were stirred for ½ an hour to isolate the solid product from the reaction mixture. The solid was separated by filtration, washed with a cold water-ethyl alcohol mixture, dried, and crystallized using alcohol to afford white compound 4 in 80% yield (mp=152-154 °C).

General procedure for the synthesis of 5-phenyl-1,3,4-thiadiazol-2-amines (3a-l)

A dry solution of POCl₃ (13 ml) was added dropwise to a mixture of **1a-l** (0.05 mol) and thiosemicarbazide (0.05 mol) at room temperature, after which the reaction mixture was heated for approximately 0.75 h at 75 °C. After cooling to room temperature, 25 ml of water was added to the reaction mixture. The reaction mixture was refluxed in a water bath for 4 h. The progress of the reaction was monitored by TLC. The reaction mixture was cooled to room temperature and basified at pH 8 by drop wise addition of 50% NaOH solution under stirring. The reaction mixture was filtered, dried and recrystallized from ethanol.

(3a) 5-Phenyl-1,3,4-thiadiazol-2-amine: white solid; yield (%): 80; mp: 242-243 °C (lit. mp 241-242 °C); IR $\nu_{\max}/\text{cm}^{-1}$: 3361 (N-H stretching), 3087 (C-H aromatic), 1613 (C=N); ^1H NMR (400 MHz, DMSO-d₆) δ 7.82-7.79 (2H, m), 7.54-7.52 (3H, m), 7.26 (2H, s); ^{13}C NMR (400 MHz, DMSO-d₆) δ 164.3, 157.7, 130.8, 129.6, 125.4, 124.8.

(3b) 2-(5-Amino-1,3,4-thiadiazol-2-yl)phenol: white solid; yield (%): 77; mp: 140-142 °C; IR $\nu_{\max}/\text{cm}^{-1}$: 3465 (O-H stretching), 3366 (N-H stretching), 3080 (C-H aromatic), 1610 (C=N); ^1H NMR (400 MHz, DMSO-d₆) δ 9.75 (1H, s, -OH), δ 7.20 (2H, s, -NH₂), δ 7.62-7.00 (5H, m); ^{13}C NMR (400 MHz, DMSO-d₆) δ 164.5, 159.1, 157.5, 127.8, 124.7, 121.8, 119.0, 117.2.

(3c) 5-(3-nitrophenyl)-1,3,4-thiadiazol-2-amine: yellow solid; yield (%): 80; mp: 252-253 °C (lit. mp 253-254 °C); IR $\nu_{\max}/\text{cm}^{-1}$: 3371 (N-H stretching), 3073 (C-H aromatic), 1617 (C=N); ^1H NMR (400 MHz, DMSO-d₆) δ 8.47 (1H, t), 8.34 (1H, dd), 8.23-8.20 (1H, m), 7.84 (1H, t), 7.47 (2H, s); ^{13}C NMR (400 MHz, DMSO-d₆) δ 164.7, 156.2, 148.6, 131.6, 131.3, 126.2, 125.1, 119.8.

(3d) 4-(5-amino-1,3,4-thiadiazol-2-yl)benzene-1,3-diol: white solid; yield (%): 80; mp: 149-151 °C; IR $\nu_{\max}/\text{cm}^{-1}$: 3472 (O-H stretching), 3355 (N-H stretching), 3062 (C-H aromatic), 1607 (C=N); ^1H NMR (400 MHz, DMSO-d₆) δ 9.81 (1H, s, -OH), 9.74 (1H, s, -OH), δ 7.23 (2H, s, -NH₂), δ 7.45-6.63 (3H, m, Ar-H); ^{13}C NMR (400 MHz, DMSO-d₆) δ 164.2, δ 157.5, 156.3, 154.8, 128.7, 114.8, 107.0, 103.5.

(3e) 4-(5-amino-1,3,4-thiadiazol-2-yl)-3-chlorophenol: white solid; yield (%): 76; mp: 209-211 °C; IR $\nu_{\max}/\text{cm}^{-1}$: 3461 (O-H stretching), 3368 (N-H stretching), 3082 (C-H aromatic), 1621 (C=N); ^1H NMR (400 MHz, DMSO-d₆) δ 9.58 (1H, s), 7.64 (1H, d), 7.52 (1H, s), 7.27 (1H, dd), 7.30 (2H, s); ^{13}C NMR (400 MHz, DMSO-d₆) δ 164.7, 157.2, 154.7, 131.7, 128.3, 127.5, 115.8, 112.4.

(3f) 4-(5-amino-1,3,4-thiadiazol-2-yl)-2-methoxyphenol: white solid; yield (%): 74; mp: 219-221 °C; IR $\nu_{\max}/\text{cm}^{-1}$: 3470 (O-H stretching), 3364 (N-H stretching), 3080 (C-H aromatic), 1618 (C=N); ^1H NMR (400 MHz, DMSO-d₆) δ 9.87 (1H, s), 7.61-7.25 (3H, m), 7.23 (2H, s), 3.83 (3H, s); ^{13}C NMR (400 MHz, DMSO-d₆) δ 164.3, 157.7, 145.8, 144.5, 124.4, 119.2, 114.3, 110.2, 55.7.

(3g) 4-(5-amino-1,3,4-thiadiazol-2-yl)-2-bromo-6-methoxyphenol: white solid; yield (%): 78; mp: 230-232 °C; IR $\nu_{\max}/\text{cm}^{-1}$: 3482 (O-H stretching), 3370 (N-H stretching), 3075 (C-H aromatic), 1601 (C=N); ^1H NMR (400 MHz, DMSO-d₆) δ 9.61 (1H, s), 7.2 (1H, s), 7.0 (1H, s), 7.34 (2H, s), 3.85 (3H, s); ^{13}C NMR (400 MHz, DMSO-d₆) δ 164.3, 158.0, 151.8, 138.3, 127.1, 124.0, 114.9, 109.6, 55.7.

(3 h) 2-(4-(5-amino-1,3-(3,4-thiadiazol-2-yl)-2-methoxyphenoxy)acetic acid: white solid; yield (%): 74; mp: 215-217 °C; IR ν_{\max} /cm $^{-1}$: 3372 (N-H stretching), 3077 (C-H aromatic), 1609 (C=N); ^1H NMR (400 MHz, DMSO-d $_6$) δ 12.21 (1H, s), δ 7.54-7.13 (3H, m, Ar-H), 7.37 (2H, s), 3.93 (3H, s), 4.72 (2H, s); ^{13}C NMR (400 MHz, DMSO-d $_6$) δ 164.7, 160.4, 157.5, 148.7, 145.1, 124.0, 118.2, 110.9, 109.5, 65.4, 55.7.

(3i) 4-(5-amino-1,3,4-thiadiazol-2-yl)-2-methoxyphenyl 2-chloroacetate: white solid; yield (%): 82; mp: 248-250 °C; IR ν_{\max} /cm $^{-1}$: 3381 (N-H stretching), 3064 (C-H aromatic), 1617 (C=N); ^1H NMR (400 MHz, DMSO-d $_6$) δ 7.57-7.14 (3H, m, Ar-H), 7.37; (2H, s), 3.92 (3H, s), 4.68 (2H, s); ^{13}C NMR (400 MHz, DMSO-d $_6$) δ 164.3, 160.7, 157.7, 148.3, 138.6, 128.2, 121.5, 118.5, 109.7, 55.1, 38.2.

(3j) 2-(5-Amino-1,3,4-thiadiazol-2-yl)phenyl acetate: white solid; yield (%): 75; mp: 229-231 °C; IR ν_{\max} /cm $^{-1}$: 3374 (N-H stretching), 3090 (C-H aromatic), 1611 (C=N); ^1H NMR (400 MHz, DMSO-d $_6$) δ 7.73-7.35 (4H, m, Ar-H), 7.33 (2H, s, -NH $_2$), 2.27 (3H, s); ^{13}C NMR (400 MHz, DMSO-d $_6$) δ 164.7, 163.2, 157.5, 148.7, 121.4, 123.7, 124.3, 127.1, 127.5, 19.4.

(3k) 5-(4-Chlorophenyl)-1,3,4-thiadiazol-2-amine: white solid; yield (%): 70; mp: 224-225 °C (lit. mp 224-226 °C); IR ν_{\max} /cm $^{-1}$: 3377 (N-H stretching), 3064 (C-H aromatic), 1632 (C=N); ^1H NMR (400 MHz, DMSO-d $_6$) δ 7.77 (2H, d), 7.53 (2H, d), 7.48 (2H, s); ^{13}C NMR (400 MHz, DMSO-d $_6$) δ 164.2, 157.5, 131.8, 130.1, 127.8, 127.3, 125.8, 125.5.

(3l) 2-(5-amino-1,3,4-thiadiazol-2-yl)-4-nitrophenol: yellow solid; yield (%): 75; mp: 199-201 °C; IR ν_{\max} /cm $^{-1}$: 3462 (O-H stretching), 3358 (N-H stretching), 3055 (C-H aromatic), 1618 (C=N); ^1H NMR (400 MHz, DMSO-d $_6$) δ 10.15 (1H, s, -OH), 8.44 (1H, t), 8.31 (1H, dd), 7.17 (1H, t), 7.27 (2H, s); ^{13}C NMR (400 MHz, DMSO-d $_6$) δ 164.5, 157.2, 156.8, 138.7, 124.3, 121.6, 121.2, 117.7.

General procedure for the synthesis of chromone-fused 1,3,4-thiadiazoles (5a-l)

To a stirred solution of 4-oxo-4*H*-chromene-3-carbaldehyde 4 (0.02 mol) in THF (5 ml) was added a solution of 5-phenyl-1,3,4-thiadiazol-2-amines 3a-l (0.02 mol) in THF (5 ml), and the resulting reaction mixture was refluxed for 3-4 h in a water bath. After the completion of the reaction (monitored by TLC), the reaction mixture was cooled to room temperature and kept overnight in a freezer. The solid was separated, filtered, dried and purified by column chromatography (ethyl acetate \times pet ether mixture: 4:6) to furnish chromone fused 1,3,4-thiadiazoles (5a-l).

5a: (*E*)-3-(((5-phenyl-1,3,4-thiadiazol-2-yl)imino)methyl)-4*H*-chromen-4-one. Yellow solid; Yield (%): 82; mp: 132-133 °C; IR_{v_{max}}/cm⁻¹: 3052, 3025 (C-H aromatic), 1655 (C=O), 1598 (C=N), 1554 (C=C), 1377 (C-O-C). ¹HNMR (400 MHz, DMSO-*d*₆) δ (ppm): 8.9 (s, 1H), 7.92-7.19 (m, 9H), 7.56 (s, 1H); ¹³CNMR (400 MHz, DMSO-*d*₆): δ 188.23, 174.78, 163.21, 136.95, 135.08, 128.68, 128.40, 127.89, 127.57, 127.25, 126.60, 126.20, 125.21, 124.80, 124.59, 119.94, 118.78, 109.01; (ESI-MS) *m/z*: 333.06 [M+H]⁺.

5b: (*E*)-3-(((5-(2-hydroxyphenyl)-1,3,4-thiadiazol-2-yl)imino)methyl)-4*H*-chromen-4-one. Pale yellow solid; yield (%): 80; mp: 142-144 °C; IR_{v_{max}}/cm⁻¹: 3067, 3045 (C-H aromatic), 1662 (C=O), 1595 (C=N), 1542 (C=C), 1368 (C-O-C). ¹HNMR (400 MHz, DMSO-*d*₆) δ (ppm): 10.15 (s, 1H, OH), 8.8 (s, 1H), 8.13-7.52 (m, 8H), 7.56 (s, 1H); ¹³CNMR (400 MHz, DMSO-*d*₆): δ 188.23, 174.78, 163.21, 155.53, 136.95, 135.08, 128.68, 128.4, 127.89, 127.57, 127.25, 126.60, 125.21, 124.80, 124.59, 119.94, 118.78, 109.01; (ESI-MS) *m/z*: 349.05 [M+H]⁺.

5C: (*E*)-3-(((5-(3-nitrophenyl)-1,3,4-thiadiazol-2-yl)imino)methyl)-4*H*-chromen-4-one. Yellow solid; Yield (%): 77; mp: 120-122 °C; IR_{v_{max}}/cm⁻¹: 3057, 3014 (C-H aromatic), 1652 (C=O), 1601 (C=N), 1549 (C=C), 1352 (C-O-C). ¹HNMR (400 MHz, DMSO-*d*₆) δ (ppm): 8.9 (s, 1H), 8.6 (s, 1H), 8.3-7.4 (m, 7H), 7.56 (s, 1H); ¹³C NMR (400 MHz, DMSO-*d*₆): δ 188.26, 169.47, 167.19, 163.26, 155.56, 148.16, 136.99, 135.11, 132.49, 132.17, 130.81, 127.61, 127.29, 126.64, 123.86, 120.31, 118.80, 109.01; (ESI-MS) *m/z*: 378.04 [M+H]⁺.

5d: (*E*)-3-(((5-(2,4-dihydroxyphenyl)-1,3,4-thiadiazol-2-yl)imino)methyl)-4*H*-chromen-4-one. Brown solid; Yield (%): 75; mp: 142-145 °C; IR_{v_{max}}/cm⁻¹: 3068, 3027 (C-H aromatic), 1670 (C=O), 1590 (C=N), 1565 (C=C), 1345 (C-O-C); ¹HNMR (400 MHz, DMSO-*d*₆) δ (ppm): 10.1-10.00 (s, 2H), 8.9 (s, 1H), 7.9-7.1 (m, 6H), 7.56 (s, 1H), 6.7 (s, 1H); ¹³CNMR (400 MHz, DMSO-*d*₆): δ 188.23, 174.78, 163.21, 138.95, 135.08, 128.68, 128.40, 127.89, 127.57, 127.25, 126.60, 126.20, 125.21, 124.80, 124.59, 119.94, 118.78, 109.01; (ESI-MS) *m/z*: 365.05 [M+H]⁺.

5e: (*E*)-3-(((5-(2-chloro-4-hydroxyphenyl)-1,3,4-thiadiazol-2-yl)imino)methyl)-4*H*-chromen-4-one. White solid; Yield (%): 75; mp: 158-160 °C; IR_{v_{max}}/cm⁻¹: 3072, 3042 (C-H aromatic), 1682 (C=O), 1587 (C=N), 1556 (C=C), 1340 (C-O-C); ¹HNMR (400 MHz, DMSO-*d*₆) δ (ppm): 10.17 (s, 1H, OH), 8.9 (s, 1H), 7.92-7.19 (m, 6H), 7.56 (s, 1H), 7.12 (s, 1H); ¹³CNMR (400 MHz, DMSO-*d*₆): δ 188.33, 174.87, 163.40, 155.61, 153.20, 137.26, 135.10, 128.75, 128.41, 127.65, 127.33, 126.72, 125.21, 124.60, 124.45, 120.05, 118.82, 109.01; (ESI-MS) *m/z*: 383.01 [M+H]⁺.

5f: (*E*)-3-(((5-(4-hydroxy-3-methoxyphenyl)-1,3,4-thiadiazol-2-yl)imino)methyl)-4*H*-chromen-4-one. Yellow solid; Yield (%): 80; mp: 189-192 °C; IR_{vmax}/cm⁻¹3058, 3022 (C-H aromatic), 2952 (CH₃), 1665 (C=O), 1585 (C=N), 1562 (C=C), 1337 (C-O-C); ¹HNMR (400 MHz, DMSO-*d*₆) δ (ppm): 10.17 (s, 1H, OH), 8.9 (s, 1H), 7.92-7.19 (m, 6H), 7.56 (s, 1H), 7.12 (s, 1H), 3.80 (s, 3H, -CH₃); ¹³C NMR (100 MHz, DMSO-*d*₆): δ188.33, 174.87, 163.40, 155.61, 137.02, 135.17, 128.75, 128.43, 127.96, 127.64, 127.32, 126.70, 125.28, 124.66, 124.46, 120.01, 118.87, 109.77, 55.78; (ESI-MS) *m/z*: 379.06 [M+H]⁺.

5g: (*E*)-3-(((5-(3-bromo-4-hydroxy-5-methoxyphenyl)-1,3,4-thiadiazol-2-yl)imino)methyl)-4*H*-chromen-4-one. Pale Yellow solid; Yield (%): 80; mp: 144-147 °C; IR_{vmax}/cm⁻¹3062, 3031 (C-H aromatic), 2955 (CH₃), 1660 (C=O), 1582 (C=N), 1547 (C=C), 1326 (C-O-C); ¹H NMR (400 MHz, DMSO-*d*₆) δ (ppm): 10.2 (s, 1H, OH), 8.9 (s, 1H), 7.92-7.19 (m, 4H), 7.56 (s, 1H), 7.1 (s, 1H), 6.85 (s, 1H), 3.83 (s, 3H, -OCH₃); ¹³CNMR (400 MHz, DMSO-*d*₆): δ188.23, 174.78, 163.21, 148.95, 137.85, 135.08, 128.68, 128.4, 127.57, 127.25, 126.60, 126.20, 125.21, 124.80, 124.59, 119.94, 118.78, 109.01, 56.1; (ESI-MS) *m/z*: 456.97 [M+H]⁺.

5h: (*E*)-2-(2-Methoxy-4-(5-(((4-oxo-4*H*-chromen-3-yl)methylene)amino)-1,3,4-thiadiazol-2-yl)phenoxy)acetic acid. Red solid; Yield (%): 80; mp: 187-188 °C; IR_{vmax}/cm⁻¹3060, 3013 (C-H aromatic), 2950 (CH₂), 1645 (C=O), 1592 (C=N), 1560 (C=C), 1349 (C-O-C); ¹HNMR (400 MHz, DMSO-*d*₆) δ (ppm):12.17 (s, 1H, OH), 8.9 (s, 1H), 7.92-7.19 (m, 6H), 7.56 (s, 1H), 7.12 (s, 1H), 4.70 (s, 2H), 3.90 (s, 3H, -OCH₃); ¹³CNMR (400 MHz, DMSO-*d*₆): δ188.45, 174.88, 163.42, 165.30, 155.65, 141.25, 137.68, 135.10, 128.75, 128.45, 127.98, 126.76, 125.24, 124.42, 120.11, 118.86, 115.26, 112.20, 109.18, 56.15, 40.20; (ESI-MS) *m/z*: 437.07[M+H]⁺.

5i: (*E*)-2-Methoxy-4-(5-(((4-oxo-4*H*-chromen-3-yl)methylene)amino)-1,3,4-thiadiazol-2-yl)phenyl-2-chloroacetate. White solid; Yield (%): 80; mp: 203-205 °C; IR_{vmax}/cm⁻¹3047, 3009 (C-H aromatic), 2958 (CH₂), 1664 (C=O), 1600 (C=N), 1562 (C=C), 1365 (C-O-C); ¹HNMR (400 MHz, DMSO-*d*₆) δ (ppm): 8.90 (s, 1H), 7.92-7.19 (m, 6H), 7.56 (s, 1H), 7.1 (s, 1H), 4.60 (s, 2H-CH₂), 3.83 (s, 3H, -OCH₃); ¹³CNMR (400 MHz, DMSO-*d*₆): δ188.45, 174.88, 163.42, 165.30, 155.65, 141.25, 137.68, 135.10, 128.75, 128.45, 127.98, 126.76, 125.24, 124.42, 120.11, 118.86, 115.26, 112.20, 109.18, 56.15, 40.20; (ESI-MS) *m/z*: 455.03 [M+H]⁺.

5j: (*E*)-2-(5-(((4-oxo-4*H*-chromen-3-yl)methylene)amino)-1,3,4-thiadiazol-2-yl)phenyl acetate. Yellow solid; Yield (%): 82; mp: 176-178 °C; IR_{vmax}/cm⁻¹3073, 3033 (C-H aromatic), 2972 (CH₂), 1659 (C=O), 1590 (C=N), 1532 (C=C), 1355 (C-O-C); ¹HNMR (400 MHz, DMSO-*d*₆) δ (ppm): 8.8 (s, 1H), 8.13-7.52 (m, 8H), 7.56 (s, 1H), 2.34 (s, 3H); ¹³CNMR (400 MHz, DMSO-*d*₆): δ188.23, 174.78, 169.45, 163.21, 155.53, 136.95, 135.08, 128.68, 128.40,

127.89, 127.57, 127.25, 126.60, 125.21, 124.80, 124.59, 119.94, 118.78, 109.01, 20.56; (ESI-MS) m/z : 391.06 [M+H]⁺.

5k: (*E*)-3-(((5-(4-Chlorophenyl)-1,3,4-thiadiazol-2-yl)imino)methyl)-4*H*-chromen-4-one. Pale yellow solid; Yield (%): 77; mp: 213-215 °C; IR_{v_{max}}/cm⁻¹3060, 3018 (C-H aromatic), 1655 (C=O), 1594 (C=N), 1542 (C=C), 1371 (C-O-C); ¹HNMR (400 MHz, DMSO-*d*₆) δ (ppm): 8.9 (s, 1H), 7.92-7.19 (m, 8H), 7.56 (s, 1H); ¹³CNMR (400 MHz, DMSO-*d*₆): δ188.33, 174.65, 168.79, 155.07, 136.96, 133.92, 131.06, 129.83, 128.64, 127.83, 127.59, 126.70, 125.25, 124.60, 124.40, 120.25, 118.80, 109.01; (ESI-MS) m/z : 367.02 [M+H]⁺.

5l: (*E*)-3-(((5-(2-hydroxy-5-nitrophenyl)-1,3,4-thiadiazol-2-yl)imino)methyl)-4*H*-chromen-4-one. Brown solid; Yield (%): 77; mp: 153-155 °C; IR_{v_{max}}/cm⁻¹3047, 3012 (C-H aromatic), 1661 (C=O), 1585 (C=N), 1552 (C=C), 1340 (C-O-C); ¹HNMR (400 MHz, DMSO-*d*₆): 10.17 (s, 1H, OH), 8.9 (s, 1H), 8.12 (s, 1H), 7.92-7.19 (m, 6H), 7.56 (s, 1H); ¹³C NMR (400 MHz, DMSO-*d*₆): δ188.33, 174.87, 163.40, 155.61, 137.02, 135.17, 128.75, 128.43, 127.96, 127.64, 127.32, 126.70, 125.28, 124.66, 124.46, 120.01, 118.87, 109.77, 55.78; (ESI-MS) m/z : 394.04 [M+H]⁺.

Acknowledgments

All the authors are grateful to University Grants Commission (UGC) for providing financial assistance. We also thank Dr. R. K. Ippar & Dr. D. V. Meshram, Principals, Jawahar Education Society's Vaidyanath College Parli-Vajinath for providing needed research facilities. We are thankful to SAIF, CDRI, Lucknow for providing spectral data.

References

- [1] S. V. Gordon and T. Parish, *Microbiology.*, 164(4), 437–439 (2018).
- [2] K. Dheda, M. Tomasicchio, A. Reuter, M. Davids, G. Calligaro, J. Furin, P. van Helden, and R. Warren, *Encyclopedia of Respiratory Medicine (Second Edition).*, 75–98 (2022).
- [3] M. G. Moule and J. D. Cirillo, *Frontiers in Cellular and Infection Microbiology.*, 10, 65 (2020).
- [4] V. Makarov, E. Salina, R. C. Reynolds, P. P. K. Zin, and S. Ekins, *Journal of Medicinal Chemistry.*, 63(17), 8917–8955 (2020).
- [5] C. Vilcheze and W. R. Jacobs, *Microbiology Spectrum.*, 2, MGM2-0014-2013 (2014).

- [6] J. Reis, A. Gaspar, N. Milhazes, and F. Borges, *Journal of Medicinal Chemistry.*, 60(19), 7941–7957 (2017).
- [7] A. B. Svendsen and J. J. C. Scheffer, *Pharmaceutisch Weekblad Scientific Edition.*, 4, 93–103 (1982).
- [8] B. A. Berman and R. N. Ross, *Clinical Reviews in Allergy.*, 1, 105–121 (1983).
- [9] M. Ceylan-Ünlüsoy, E. J. Verspohl, and R. Ertan, *Journal of Enzyme Inhibition and Medicinal Chemistry.*, 25(6), 784–789 (2010).
- [10] H. M. Hiruy, D. Bisrat, A. Mazumder, and K. Asres, *Natural Product Research.*, 35(6), 1052–1056 (2021).
- [11] C. F. Silva, D. C. Pinto, and A. M. Silva, *ChemMedChem.*, 11(20), 2252–2260 (2016).
- [12] J. Reis, A. Gaspar, N. Milhazes, and F. Borges, *Journal of Medicinal Chemistry.*, 60(19), 7941–7957 (2017).
- [13] K. C. Rajanna, F. Solomon, M. M. Ali, and P. K. Saiprakash, *Tetrahedron.*, 52(10), 3669–3682 (1996).
- [14] D. Ameen and T. J. Snape, *Synthesis.*, 47(2), 141–158 (2015).
- [15] D. A. Williams, C. Smith, and Y. Zhang, *Tetrahedron Letters.*, 54(32), 4292–4295 (2013).
- [16] I. T. Hwang, S. A. Lee, J. S. Hwang, and K. I. Lee, *Molecules.*, 16(8), 6313–6321 (2011).
- [17] E. Petschek and H. Simonis, *Berichte der Deutschen Chemischen Gesellschaft.*, 46, 2014 (1913).
- [18] J. W. Zhang, W. W. Yang, L. L. Chen, P. Chen, Y. B. Wang, and D. Y. Chen, *Organic and Biomolecular Chemistry.*, 17, 7461–7467 (2019).
- [19] S. Maddila, S. Gorle, C. Sampath, and P. Lavanya, *Journal of Saudi Chemical Society.*, 20(1), S306–S312 (2016).
- [20] S. Turner, M. Myers, B. Gadie, A. J. Nelson, R. Pape, J. F. Saville, J. C. Doxey, and T. L. Berridge, *Journal of Medicinal Chemistry.*, 31(5), 902–906 (1988).
- [21] A. A. Othman, M. Kihel, and S. Amara, *Arabian Journal of Chemistry.*, 12(7), 1660–1675 (2019).
- [22] E. E. Oruç, S. Rollas, F. Kandemirli, N. Shvets, and A. S. Dimoglo, *Journal of Medicinal Chemistry.*, 47(27), 6760–6767 (2004).
- [23] M. R. Stillings, A. P. Welbourn, and D. S. Walter, *Journal of Medicinal Chemistry.*, 29(11), 2280–2284 (1986).

- [24] M. N. Noolvi, H. M. Patel, S. Kamboj, and S. S. Cameotra, *Arabian Journal of Chemistry*., 9(2), S1283–S1289 (2016).
- [25] J. Matysiak, *Mini Reviews in Medicinal Chemistry*., 15(9), 762–775 (2015).
- [26] R. F. Rodrigues, K. S. Charret, E. F. da Silva, A. Echevarria, V. F. Amaral, L. L. Leon, and M. M. Canto-Cavalheiro, *Antimicrobial Agents and Chemotherapy*., 53(2), 839–842 (2009).
- [27] a) V. A. Obakachi, B. Kushwaha, N. D. Kushwaha, S. Mokoena, A. M. Ganai, T. K. Pathan, W. E. van Zyl, and R. Karpoomath, *Journal of Sulfur Chemistry*., 42(6), 670–691 (2021); b) D. Chandra Sekhar, D. V. Venkata Rao, and A. Tejeswara Rao, *Russian Journal of General Chemistry*., 89, 770–779 (2019).
- [28] K. Brodowska and E. Lodyga-Chruscinska, *Chemik*., 68(2), 129–134 (2014).
- [29] L. Kaviarasan, B. Gowramma, R. Kalirajan, M. Mevithra, and S. Chandralekha, *Journal of the Iranian Chemical Society*., 17(8), 2083–2094 (2020).
- [30] a) L. B. Leonard, J. Coronel, M. Siedner, L. Grandjean, L. Caviedes, P. Navarro, R. H. Gilman, and D. A. J. Moore, *Journal of Clinical Microbiology*., 46(10), 3526–3529 (2008); b) C. Ryan, B. T. Nguyen, and S. J. Sullivan, *Journal of Clinical Microbiology*., 33(7), 1720–1726 (1995).
- [31] I. Li de la Sierra, H. Munier-Lehmann, A. M. Gilles, O. Bârzu, and M. Delarue, *Journal of Molecular Biology*., 311(1), 87–100 (2001).
- [32] E. Morgunova, W. Meining, B. Illarionov, I. Haase, G. Jin, A. Bacher, M. Cushman, M. Fischer, and R. Ladenstein, *Biochemistry*., 44(8), 2746–2758 (2005).
- [33] C. Vilchèze, H. R. Morbidoni, T. R. Weisbrod, H. Iwamoto, M. Kuo, J. C. Sacchettini, and W. R. Jacobs Jr., *Journal of Bacteriology*., 182, 4059–4067 (2000).
- [34] E. Dhamija, S. Yabaji, A. Chatterjee, A. Mishra, R. K. Dubey, A. Narain, and K. K. Srivastava, *European Respiratory Journal*., 54(Suppl. 63), PA4592 (2019).
- [35] T. A. Halgren, R. B. Murphy, R. A. Friesner, H. S. Beard, L. L. Frye, W. T. Pollard, and J. L. Banks, *Journal of Medicinal Chemistry*., 47, 1750–1759 (2004).
- [36] K. Mdluli and M. Spigelman, *Current Opinion in Pharmacology*., 6, 459–467 (2006).
- [37] A. Daina, O. Michielin, and V. Zoete, *Scientific Reports*., 7, 42717 (2017). [38] C. A. Lipinski, F. Lombardo, B. W. Dominy, and P. J. Feeney, *Advanced Drug Delivery Reviews*., 46(1–3), 3–26 (2001).
- [39] a) K. T. Savjani, et al., *ISRN Pharmaceutics*., (2012); b) J. A. Arnot and S. L. Planey, *Expert Opinion on Drug Discovery*., (2012).
- [40] D. E. Clark, *Journal of Pharmaceutical Sciences*., 88, 815–821 (1999).

[41] P. R. Twentyman and M. Luscombe, British Journal of Cancer., 56, 279–285 (1987).

HOW TO CITE THIS ARTICLE

Babasaheb V Kendre; Pawan S Hardas; Rajashri c Pat; Rushikesh B Kendre; Mahadev G Landge; Sudhakar R Bhusare. "**Design, Synthesis and Biological Evaluation of Chromone Fused 1,3,4-Thiadiazoles as Highly Potent Nontoxic Inhibitors of Enoyl-Acyl Carrier Proteins in M. tuberculosis**", International Journal of New Chemistry, 2025; 12(4), 581-606. doi: 10.22034/ijnc.2024.2020026.1369